J. Fluid Mech. (2005), *vol.* 540, *pp.* 39–48.
doi:10.1017/S0022112005006099 Printed in the United Kingdom

On intermittency and the physical thickness of turbulent fluid interfaces

By ROBERTO C. AGUIRRE AND HARIS J. CATRAKIS

Iracletos Flow Dynamics and Turbulence Laboratories
Mechanical and Aerospace Engineering, University of California, Irvine, CA 92697, USA

(Received 3 September 2004 and in revised form 3 July 2005)

The variability of the physical thickness of fully developed turbulent interfaces is examined using scalar measurements in the outer far-field regions of round jets at a Reynolds number of $Re \sim 20\,000$ and Schmidt number of $Sc \sim 2000$. The interfacial thickness is considered in terms of the inverse magnitude of the scalar gradient across the interface and its relation to the scalar dissipation rate. The thickness variations and their conditional statistics are examined on outer interfaces at a resolution of $\sim 1000^3$ with data that capture the full transverse extent of the flow. At the resolution of the present measurements, the interfaces are observed to exhibit highly intermittent thickness variations that consist of striation patterns, or undulations, along the interfacial surfaces. The conditional probability density of the interfacial thickness is found to be nearly lognormal, in agreement with previous studies. A new scale-local density measure of the interfacial thickness is formulated to examine the effects of coarse graining and the dependence of the thickness on resolution scale. The scale-local thickness density, conditionally averaged on the outer interfaces, is found to exhibit self-similarity in a range of resolved scales. This observation of self-similar behaviour, in conjunction with intermittency, provides a physical ingredient useful for studies of phenomena sensitive to turbulent interfaces.

1. Introduction

Knowledge of the behaviour of turbulent fluid interfaces, such as scalar interfaces generated in large-Reynolds-number flows, is useful in a variety of basic and applied problems (e.g. Pope 1988, 2000; Sreenivasan 1991, 1999, 2004; Warhaft 2000; Catrakis 2004). This is because physical, chemical or biological effects often occur across or on such interfaces, e.g. molecular diffusion, electromagnetic-/optical-wave propagation, chemical reactions or bioluminescence (e.g. Villermaux & Innocenti 1999; Bilger 2004; Latz *et al.* 2004; Dimotakis 2005; Schumacher, Sreenivasan & Yeung 2005). As a result, it is desirable to develop an understanding of the physical aspects of such interfaces in problems ranging from aeronautical flows to biological flows. Fundamentally, interfacial properties provide clues to the distribution of physical scales in turbulence (e.g. Sreenivasan, Prabhu & Narasimha 1983; Catrakis 2000). Depending on the problem, different interfacial properties are useful for the development of physical models. Examples of properties examined in previous works include scale-local and scale-cumulative quantities such as fractal dimensions, the area–volume ratio or surface density, the probability density of level-crossing scales or spacings, the spectral behaviour, and multifractal measures (e.g. Sreenivasan 1991; Trouvé & Poinsot 1994; Schumacher & Sreenivasan 2003). Because turbulent interfaces have

highly irregular structure, especially at large Reynolds numbers, challenges persist in their examination, modelling, and optimization.

The term 'turbulent interface' is often used to denote various types of turbulence-generated fluid interfaces, some of which are related to intermittency. Interfaces are referred to as 'isosurfaces', 'layers' or 'fronts' and may exhibit diffusive or non-diffusive properties. These include concentration, density, or other scalar interfaces as well as level crossings of velocity-component signals (e.g. Sreenivasan *et al.* 1983; Sreenivasan, Ramshankar & Meneveau 1989; Villermaux & Innocenti 1999). External intermittency refers to turbulent/non-turbulent interfaces such as the outer vorticity or scalar interfaces (e.g. LaRue & Libby 1975; Bisset, Hunt & Rogers 2002). Internal intermittency refers to the variability of the energy or scalar dissipation rates (e.g. Sreenivasan 1985; Bilger 2004; Schumacher *et al.* 2005). The turbulent/non-turbulent vorticity interface denotes the outer boundary between vortical and irrotational fluid, also known as the 'turbulence front' (e.g. Corrsin & Kistler 1955; Bisset *et al.* 2002). The outer scalar interface denotes the interface between mixed fluid and pure fluid (e.g. Joseph & Preziosi 1989; Catrakis *et al.* 2002*b*). Prior work on external intermittency includes studies of the dynamics and correlations of outer vorticity and scalar interfaces (e.g. Bisset *et al.* 2002; Catrakis *et al.* 2002*b*). Previous work on internal intermittency includes studies of the probability density of the scalar dissipation rate in various flows (e.g. Antonia & Sreenivasan 1977; Sreenivasan 1985; Dahm & Southerland 1997; Su & Clemens 1999), findings on multifractal aspects of the energy and scalar dissipation rates (e.g. Meneveau & Sreenivasan 1991; Sreenivasan 1991), examinations of joint statistics of scalar fields and dissipation rates (e.g. Anselmet, Djeridi & Fulachier 1994), and studies of the geometrical structure of active dissipation regions (e.g. Sreenivasan 1999; Brethouwer, Hunt & Nieuwstadt 2003; Schumacher & Sreenivasan 2003; Schumacher *et al.* 2005).

In the present work, the intermittency of the physical thickness of outer scalar interfaces is examined. A database that captures the full transverse extent of the far field of round jets above the mixing transition is utilized. This facilitates the study of conditional statistics, for fully developed outer interfaces, but has resolution limitations compared to local measurements or direct numerical simulations (e.g. Sreenivasan 1985; Dahm & Southerland 1997; Schumacher *et al.* 2005). While the present data are resolution limited and provide coarse-grained scalar field information, they enable a study of variable-resolution effects above the image-resolution scale. In § 2, a scale-local density measure of the interfacial thickness is introduced which enables a study of resolution-scale effects on the coarse-grained scalar field. In § 3, the thickness variations and their conditional statistics are examined on the outer scalar interfaces. Quantitative visualizations of the thickness variations are presented. Conditional statistics for the scale-local density of the mean interfacial thickness indicate self-similar structure over a range of resolved scales. This finding on the interfacial thickness density, together with knowledge of the interfacial-area density (e.g. Catrakis, Aguirre & Ruiz-Plancarte 2002*a*), provides a useful ingredient for physical modelling and subgrid-scale modelling as discussed in the conclusions.

2. The role of the physical thickness of turbulent interfaces

Fluid interfaces have previously been viewed primarily as corresponding to isosurfaces of flow-field quantities, e.g. $q(\boldsymbol{x}, t)$, which can be chosen as scalar valued and dimensionless without loss of generality. Examples of $q(\boldsymbol{x}, t)$ are diffusive or non-diffusive quantities such as concentration, density, or vorticity magnitude. Such

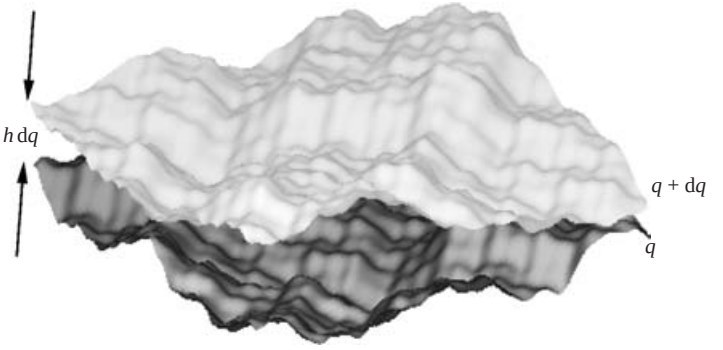

FIGURE 1. Three-dimensional schematic of the interfacial thickness $h(\boldsymbol{x}, t)\,\mathrm{d}q$ corresponding to a scalar-valued field of interest $q(\boldsymbol{x}, t)$. The interfacial thickness is quantified as the spacing between the neighbouring isosurfaces corresponding to the thresholds $q + \mathrm{d}q$ and q, as shown.

flow-field isosurfaces, i.e.

$$q(\boldsymbol{x}, t) = \text{const.}, \tag{2.1}$$

have zero thickness mathematically. However, physically, it is essential to appreciate that the corresponding fluid interfaces must exhibit in general a finite thickness.

The role of the physical thickness of turbulent interfaces can be appreciated by interpreting geometrically the probability density function (p.d.f.) of the field $q(\boldsymbol{x}, t)$, as indicated in figure 1. The probability $p(q)\,\mathrm{d}q$ is the differential volume fraction of fluid contained within the two neighbouring isosurfaces $q + \mathrm{d}q = \text{const.}$ and $q = \text{const.}$ The differential volume between the two isosurfaces can be expressed as $A(q)\,\overline{h}(q)\,\mathrm{d}q$ such that the p.d.f. $p_q(q)$ is directly determined by the interfacial properties as

$$p_q(q) \equiv \frac{\langle A(q)\overline{h}(q)\rangle_q}{V_{\mathrm{ref}}}, \tag{2.2}$$

where $\langle\cdot\rangle_q$ denotes the conditional statistic of ensemble averaging on interfaces, $A(q)$ denotes the interfacial surface area and $\overline{h}(q)$ is the mean inverse scalar gradient across the interface (cf. Kuznetsov & Sabel'nikov 1990; Bilger 2004). The latter quantity is also useful as a measure of the mean interfacial thickness, as discussed below. The contribution from the differential volume, in (2.2), is normalized by the volume V_{ref} of a reference region in which the p.d.f. has the normalization $\int_{q_{\min}}^{q_{\max}} p_q(q)\,\mathrm{d}q = 1$, with the values $q_{\min} \leqslant q \leqslant q_{\max}$ corresponding to the variations in the reference region of volume V_{ref}.

To quantify the interfacial thickness, various measures can be used (e.g. Sreenivasan *et al.* 1989; Bisset *et al.* 2002). In this work, we consider the thickness in terms of the inverse of the magnitude of the gradient of q across the interface, denoted as $h(\boldsymbol{x}, t)$:

$$h(\boldsymbol{x}, t) \equiv \frac{1}{|\nabla q(\boldsymbol{x}, t)|} = \left|\frac{\partial q}{\partial n}\right|^{-1}, \tag{2.3}$$

where $|\nabla q|$ is the magnitude of the gradient across the interface and n denotes distance along the gradient. For a differential value $\mathrm{d}q$, the thickness is $h(\boldsymbol{x}, t)\,\mathrm{d}q$ and corresponds to the spacing between neighbouring isosurfaces as illustrated in figure 1. The quantity $h(\boldsymbol{x}, t)$ is, strictly speaking, the interfacial thickness per unit value of the dimensionless flow quantity q. For simplicity we will refer to $h(\boldsymbol{x}, t)$ as the interfacial thickness.

For each interface, the mean thickness $\overline{h}(q)$ in the geometrical interpretation of the p.d.f. in equation (2.2) is the average value over the interfacial surface S_q, i.e.

$$\overline{h}(q) \equiv \frac{1}{A(q)} \int\int_{S_q} h(\boldsymbol{x}, t)\, \mathrm{d}A = \frac{1}{A(q)} \int\int_{S_q} \left| \frac{\partial q}{\partial n} \right|^{-1} \mathrm{d}A. \tag{2.4}$$

The gradient ∇q is normal to the interface at all locations on the interfacial surface. As long as the gradient magnitude $|\nabla q|$ is finite, the interfacial thickness must also be finite. By examining and combining (2.2) and (2.4), an interesting observation follows in that the interfacial thickness variations alone directly determine the p.d.f. $p_q(q)$, i.e.

$$p_q(q) \equiv \frac{1}{V_{\mathrm{ref}}} \left\langle \int\int_{S_q} h(\boldsymbol{x}, t)\, \mathrm{d}A \right\rangle_q. \tag{2.5}$$

Equations (2.2)–(2.5), are written assuming the local thickness is finite. If there are any regions of the flow where $|\nabla q| = 0$, i.e. if there are regions with no variations in q, then these relations can be modified in terms of the spatial extent of such regions (e.g. Catrakis 2004).

In practice, for large-Reynolds-number flows, it is difficult to attain the necessary resolution to capture accurately and directly the full range of scales in experiments or computations. However, with experimental data, one can still conduct coarse graining *a posteriori* at variable scales above the resolution scale. To do so, it is helpful to appreciate the idea of scale-cumulative vs. scale-local effects (e.g. Catrakis *et al.* 2002*a*) wherein the interfacial behaviour coarse-grained at a scale λ reflects only the features at or above that scale. Thus, in addition to the full-resolution p.d.f. $p_q(q)$, it is useful to consider the coarse-grained p.d.f. $p_{q;\lambda}(q;\lambda)$ corresponding to a resolution scale λ as

$$p_{q;\lambda}(q;\lambda) \equiv \frac{\langle A(q;\lambda)\, \overline{h}(q;\lambda) \rangle_q}{V_{\mathrm{ref}}}, \tag{2.6}$$

cf. (2.2), where $A(q;\lambda)$ is the coarse-grained interfacial surface area and $\overline{h}(q;\lambda)$ is the mean coarse-grained interfacial thickness. These two coarse-grained quantities can each be expressed as integrals of the scale-local contributions, i.e. in terms of the contributions as a function of scale, by introducing the respective scale-local densities, e.g.

$$A(q;\lambda) \equiv A(q;\lambda_{\min}) - \int_{\lambda_{\min}}^{\lambda} g_A(q;\lambda')\, \mathrm{d}\lambda' \quad \text{or} \quad g_A(q;\lambda) \equiv -\frac{\mathrm{d}A(q;\lambda)}{\mathrm{d}\lambda}, \tag{2.7}$$

where $g_A(q;\lambda)$ is the scale-local surface area density, and

$$\overline{h}(q;\lambda) \equiv \overline{h}(q;\lambda_{\min}) + \int_{\lambda_{\min}}^{\lambda} g_{\overline{h}}(q;\lambda')\, \mathrm{d}\lambda' \quad \text{or} \quad g_{\overline{h}}(q;\lambda) \equiv \frac{\mathrm{d}\,\overline{h}(q;\lambda)}{\mathrm{d}\lambda}, \tag{2.8}$$

where $g_{\overline{h}}(q;\lambda)$ is the scale-local mean interfacial thickness density. The surface area and mean interfacial thickness, at a fully resolved scale $\lambda_{\min}$, are denoted as $A(q;\lambda_{\min})$ and $\overline{h}(q;\lambda_{\min})$ respectively. In previous studies, coarse-graining aspects of the surface area were examined (e.g. Catrakis *et al.* 2002*a*). Here, the behaviour of the coarse-grained interfacial thickness and the role of intermittency will be examined (§ 3).

For diffusive fields, it is also useful to consider the square magnitude of the gradient of q across each interface, which contributes to the conditional mean scalar dissipation rate in the case of mixing (e.g. Pope 2000). This can be denoted as $\zeta(\boldsymbol{x}, t)$, i.e.

$$\zeta(\boldsymbol{x}, t) \equiv |\nabla q(\boldsymbol{x}, t)|^2 = h^{-2}(\boldsymbol{x}, t), \tag{2.9}$$

recalling equation (2.3). In other words, the interfacial thickness $h(\boldsymbol{x}, t)$ is

$$h(\boldsymbol{x}, t) = \zeta^{-1/2}(\boldsymbol{x}, t). \tag{2.10}$$

For example, in turbulent mixing, ζ is related to the scalar dissipation rate χ as $\zeta = \chi/\mathscr{D}$ since $\chi \equiv \mathscr{D}\,|\nabla c|^2$, with $q = c(\boldsymbol{x}, t)$ for the scalar field and $\mathscr{D}$ for the scalar diffusivity. The thickness is in this case $h = \sqrt{\mathscr{D}/\chi}$, i.e. it is the strain-limited diffusion-layer thickness (e.g. Sreenivasan *et al.* 1989). The p.d.f. of such thickness variations along an interface is a conditional statistic requiring knowledge of the interfacial location.

3. Examination of fully developed interfacial thickness variations

In order to contribute to studies of interfacial thickness variations in large-Reynolds-number flows, it is recognized that one needs to examine turbulence at fully developed flow conditions (e.g. Roshko 1991). This is because at such conditions one may anticipate various manifestations of self-similarity (e.g. Sreenivasan 1999) which provides the means to extrapolate to larger Reynolds numbers. For this reason, we will utilize the database of turbulent scalar interfaces previously recorded and described in Catrakis *et al.* (2002*b*). Those measurements, while resolution limited, span the full transverse extent of fully developed interfaces and enable a study of the coarse-grained behaviour of the thickness variations along the interfaces. A brief summary of the experiments is included here, for completeness, along with a discussion on resolution limitations.

The data consist of scalar measurements in the far field of round jets at a Reynolds number of $Re \sim 20\,000$, a Schmidt number of $Sc \sim 2000$ and a downstream distance of $z/d \sim 500$ jet-nozzle diameters. The imaging was conducted at a fixed downstream location in the similarity plane of the flow. Sets of approximately 1000 temporally consecutive scalar-field images were recorded during each experiment at an imaging rate matching the mean velocity U_{outer} of the outer scalar interfaces separating mixed fluid from pure ambient fluid. The spatial resolution of each two-dimensional spatial image is $\sim 1000 \times 1000$ pixels, so that each three-dimensional space–time data set spans a volume of approximately 1000^3 data values. The large-scale transverse extent is $L \sim 0.5$ m and the resolution scale resulting from the number of pixels as well as the laser-sheet thickness is $\lambda_{\mathrm{res}} \sim 500\,\mu$m, i.e. $L/\lambda_{\mathrm{res}} \sim 10^3$. Based on the energy dissipation rate on the centreline of jets (e.g. Friehe, Van Atta & Gibson 1971), the Kolmogorov scale is $\lambda_{\mathrm{K}} \simeq 0.95\, Re^{-3/4}\, L \simeq 600\,\mu$m and the Batchelor scale is $\lambda_{\mathrm{B}} = \lambda_{\mathrm{K}}\, Sc^{-1/2} \simeq 10\,\mu$m. Thus, at least in terms of jet-centreline estimates, the limited resolution of the present database can only capture those scales that are larger than the Kolmogorov scale. Nevertheless, the database enables an *a posteriori* examination of coarse-graining properties, above the resolution scale, such as the scale-local mean interfacial thickness density, cf. (2.8). For the behaviour at very fine scales, i.e. scales smaller than the Kolmogorov scale, we refer the reader to recent direct numerical simulations conducted with full resolution at reduced Reynolds numbers (Schumacher *et al.* 2005).

To evaluate and quantitatively visualize the conditional behaviour of the thickness variations, along the outer scalar interfaces, the full scalar gradient would be needed. In the present data, the out-of-plane scalar gradient component can only be estimated. In order to attempt this, we utilize Taylor's hypothesis keeping in mind however that in the outer regions of the jet near the turbulent/non-turbulent vorticity interface there may be possible occurrences of flow reversal (e.g. Dahm & Southerland 1997; Su & Clemens 1999; Pope 2000; Bisset *et al.* 2002), i.e.

$$\widetilde{h}(q_1) \equiv \frac{h(q_1)}{\langle \overline{h}(q_1) \rangle} \quad \text{with} \quad h(q_1) = \frac{1}{|\nabla q_1|} \;\simeq\; \left| \left(\frac{\partial q_1}{\partial x}, \frac{\partial q_1}{\partial y}, \frac{1}{U_{\mathrm{outer}}} \frac{\partial q_1}{\partial t} \right) \right|^{-1}, \tag{3.1}$$

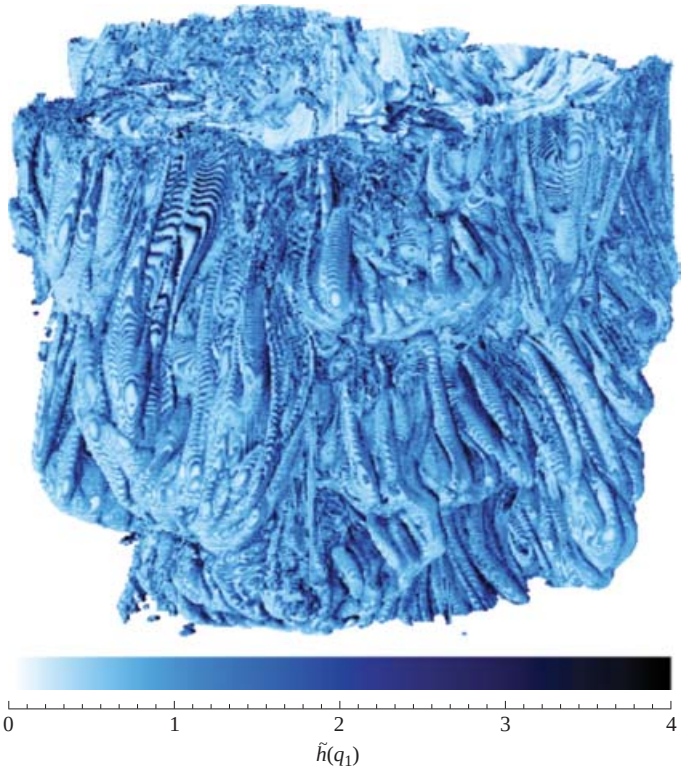

FIGURE 2. Quantitative visualization at a whole-field resolution of $\sim 1000^3$ of the variations in the interfacial thickness $\widetilde{h}(q_1)$ along a fully developed outer scalar interface at $Re \sim 20\,000$ and $Sc \sim 2000$. The colours, ranging from light blue to dark blue, denote increasing values of the interfacial thickness or decreasing values of the scalar gradient magnitude.

where $h(q_1)$ denotes the set of conditional thickness values evaluated for the normalized dimensionless scalar threshold q_1 of the outer interfaces (cf. Catrakis *et al.* 2002*b*), and $\widetilde{h}(q_1)$ denotes these values normalized by the ensemble-averaged conditional mean thickness $\langle \overline{h}(q_1) \rangle$. While the flow-imaging rate matches the mean velocity U_{outer} of the outer interfaces, the velocity fluctuations of these interfaces are probably of significant magnitude relative to U_{outer}. To gauge the applicability of Taylor's hypothesis, for estimating the interfacial thickness, we consider below the p.d.f. of the estimated conditional scalar dissipation rate which is directly related to the p.d.f. of the thickness, cf. (2.10).

The variability of the interfacial thickness is demonstrated in the example of the quantitative visualization in figure 2. Locally thin regions of the interface are labelled with light blue, and locally thick regions with dark blue. It is evident, on the basis of multiple visualizations such as in figure 2, that the outer interfaces exhibit thickness variations along the entire interfacial surfaces. These thickness variations are seen to consist of striation patterns, or undulations, along the interfaces. In some regions, these striation patterns appear to exhibit nearly one-dimensional or axisymmetric local structure. However, more complicated topologies are also present in other regions. The highly intermittent nature of the thickness is apparent with multiple regions exhibiting thickness values that are significantly smaller or larger than the mean interfacial thickness. The variability in the thickness reflects the intermittency of the scalar dissipation-rate field and the strain-rate field on the interfaces. Locally thin

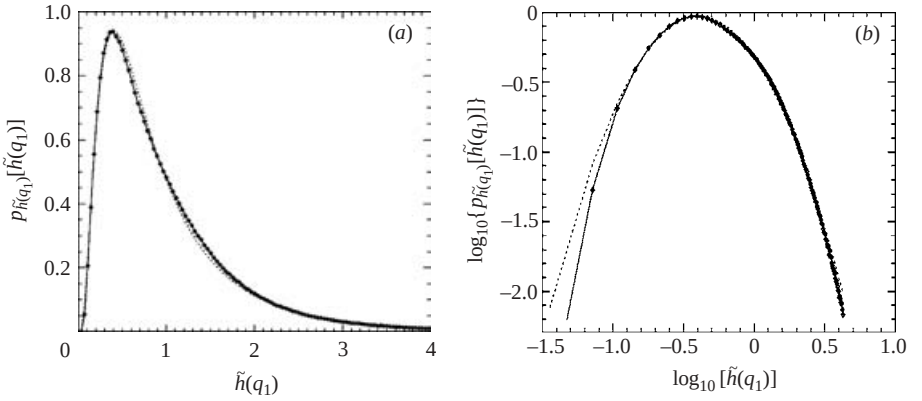

FIGURE 3. (*a*) Conditional probability density $p_{\tilde{h}(q_1)}[\widetilde{h}(q_1)]$ of the thickness variations of outer scalar interfaces for the present data, at the same flow conditions as for figure 2. Solid curve with symbols is for the measurements. Dotted curve is the lognormal model. (*b*) Double-logarithmic coordinate behaviour of the conditional probability density with the solid curve and symbols for the data and the dotted curve for the lognormal model.

regions of the interfaces correspond to active regions with high scalar dissipation rate and high strain rate. The present observations are consistent with previous findings on the structure of intermittency since the striation patterns along the interfaces can be interpreted as the interfacial intersections of sheet-like active regions that have previously been observed in studies of dissipation-rate fields (e.g. Sreenivasan 1985; Brethouwer *et al.* 2003).

From the interfacial thickness data, the conditional p.d.f. $p_{\tilde{h}(q_1)}[\widetilde{h}(q_1)]$ of the thickness along the outer interfaces was evaluated. This was computed as an ensemble average over several realizations at the same flow conditions as for the visualization in figure 2. The conditional p.d.f. is shown in figure 3 in linear coordinates as well as in double-logarithmic coordinates. Over a relatively wide range of thickness variations, the measurements suggest that the conditional-p.d.f. behaviour can be approximated well by lognormal statistics. Specifically, in the range $-1.0 \lesssim \log_{10}[\widetilde{h}(q_1)] \lesssim 0.65$ the measurements agree closely with the lognormal model shown as a dotted curve in figure 3:

$$p_{\tilde{h}(q_1)}[\widetilde{h}(q_1)] \simeq \frac{1}{\sigma_{\tilde{h}}(2\pi)^{1/2}\widetilde{h}(q_1)} \exp\left\{-\frac{1}{2}\left[\frac{1}{\sigma_{\tilde{h}}}\ln\widetilde{h}(q_1) + \frac{\sigma_{\tilde{h}}}{2}\right]^2\right\}. \tag{3.2}$$

The normalization of the interfacial thickness by its mean value $\overline{h}(q_1)$ results in a one-parameter fit with $\sigma_{\tilde{h}} \simeq 0.78$ for the present flow conditions. At low thickness values, the observed deficit in probability density is probably due to the resolution limitations.

In the general case, the p.d.f. of the interfacial thickness is directly related to the p.d.f. of the square magnitude $\zeta = 1/h^2$ of the scalar gradient, cf. (2.10). The two conditional p.d.f.s must always be such that $p_h[h(q)]\,|\mathrm{d}h| = p_\zeta[\zeta(q)]\,|\mathrm{d}\zeta|$, by conservation of probability. Thus, in terms of the normalized variables $\widetilde{h} \equiv h/\langle\overline{h}\rangle$ and $\widetilde{\zeta} \equiv \zeta/\langle\overline{\zeta}\rangle$:

$$p_{\tilde{h}(q_1)}[\widetilde{h}(q_1)] = p_{\tilde{\zeta}(q_1)}[\widetilde{\zeta}(q_1)]|\mathrm{d}\widetilde{\zeta}/\mathrm{d}\widetilde{h}| \quad \text{with} \quad |\mathrm{d}\widetilde{\zeta}/\mathrm{d}\widetilde{h}| = 2\,\widetilde{\zeta}(q_1)/\widetilde{h}(q_1), \tag{3.3}$$

expressed here for the outer-interface threshold q_1. These relations have an interesting consequence for interfaces exhibiting lognormal behaviour. Namely, combining (3.2) and (3.3) shows that lognormal statistics of the thickness must imply similar statistics for the square magnitude ζ of the scalar gradient or the scalar dissipation

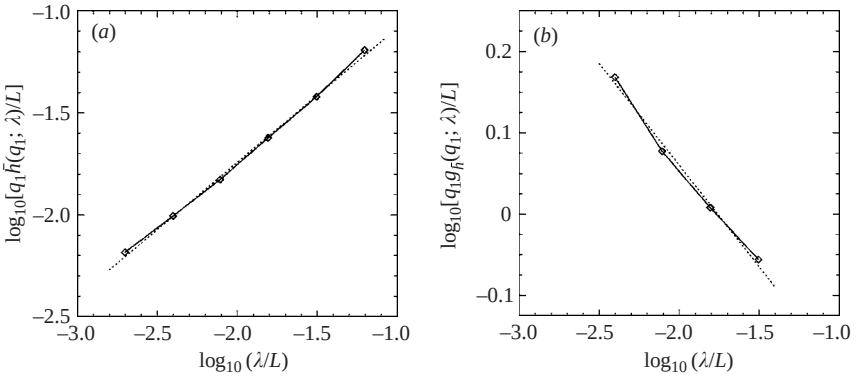

FIGURE 4. (*a*) Resolution-scale dependence of the mean coarse-grained interfacial thickness $\overline{h}(q_1;\lambda)$ for outer interfaces, where the resolution scale λ is normalized by the large scale L of the interfaces. (*b*) Scale-local interfacial thickness density $g_{\overline{h}}(q_1;\lambda)$ vs. normalized resolution scale λ/L. Solid curves and symbols are for the data. Dotted curves are power-law models.

rate $\chi = \mathscr{D}\zeta$, and vice versa. The relation between the corresponding parameters is $\sigma_{\tilde{\zeta}} = 2\sigma_{\tilde{h}}$. The observed behaviour in figure 3, therefore, is consistent with previous findings of lognormal statistics of the scalar dissipation rate (e.g. Antonia & Sreenivasan 1977; Sreenivasan 1985; Bilger 2004) and, furthermore, indicates that the conditional p.d.f.s along the interfaces also exhibit lognormal statistics. The results in figure 3, therefore, represent the intermittency effect along the interfaces.

As indicated in § 2, on the basis of the general considerations in (2.2) for the p.d.f. $p_q(q)$ of flow-derived fields, the mean interfacial thickness $\overline{h}(q)$ is a useful quantity for physical modelling. Also, for large-Reynolds-number flows, there are usually resolution limitations associated with attempting to capture directly the full range of interfacial thickness variations. For example, in the present database, direct whole-field imaging of the interfaces is restricted to finite resolution which results in averaging over the under-resolved scales. For these reasons, it is helpful to conduct *a posteriori* coarse graining of the scalar field and to examine resolution-scale effects on the mean interfacial thickness, as discussed in (2.8). Figure 4(*a*) shows the dependence on resolution scale λ for the mean coarse-grained interfacial thickness $\overline{h}(q_1;\lambda)$ of the outer interfaces. The present database was successively coarse grained and, at each resolution level, the mean interfacial thickness $\overline{h}(q_1;\lambda)$ was evaluated. The data indicate a power-law dependence of the mean interfacial thickness on resolution scale

$$\overline{h}(q_1;\lambda) \sim \left(\frac{\lambda}{L}\right)^{\alpha}, \tag{3.4}$$

with an exponent of $\alpha \simeq 0.66$ for the present flow conditions. This behaviour corresponds to cumulative contributions from interfacial scales. Namely, the mean coarse-grained interfacial thickness $\overline{h}(q_1;\lambda)$ consists of contributions at scales greater than or equal to λ, i.e. scales spanning the variable scale λ to the largest extent L of the interfaces. It is helpful, therefore, to distinguish between the scale-local and cumulative contributions. This can be done in terms of the scale-local interfacial thickness density $g_{\overline{h}}(q_1;\lambda)$, as defined in (2.8). Its dependence on resolution scale is shown in figure 4(*b*):

$$g_{\overline{h}}(q_1;\lambda) \sim \left(\frac{\lambda}{L}\right)^{\alpha-1} \quad \text{with} \quad \overline{h}(q_1;\lambda) = \overline{h}(q_1;\lambda_{\min}) + \int_{\lambda_{\min}}^{\lambda} g_{\overline{h}}(q_1;\lambda')\,\mathrm{d}\lambda', \tag{3.5}$$

i.e. the scale-local density is also a power law since it is a derivative of the cumulative quantity with respect to scale, cf. (2.8) and (3.4). This indicates self-similarity in the scale-local contributions to the mean interfacial thickness, which enables modelling of the subgrid-scale integral term in (3.5). Together with knowledge of the surface-area scale-local contributions (e.g. Catrakis *et al.* 2002*a*), the present finding is useful therefore for incorporating resolution-scale effects in physical models including subgrid-scale modelling approaches (e.g. Pullin & Saffman 1998; Meneveau & Katz 2000).

4. Conclusions

The variability of the thickness of fully developed turbulent interfaces has been examined using whole-field scalar measurements at a resolution of $\sim 1000^3$ in the outer far-field regions of round jets at a Reynolds number of $Re \sim 20\,000$ and Schmidt number of $Sc \sim 2000$. Interfacial-thickness striation patterns, or undulations, were found along the interfacial surfaces on the basis of quantitative visualizations. This is consistent with previous observations of sheet-like structures in the scalar dissipation-rate field (e.g. Sreenivasan 1985; Brethouwer *et al.* 2003). The conditional probability density of the thickness variations along the interfaces was found to be nearly lognormal in accord with previous studies of the dissipation rate (e.g. Antonia & Sreenivasan 1977; Sreenivasan 1985; Bilger 2004). While the present data are resolution limited, they have enabled an examination of variable-resolution effects above the image-resolution scale by coarse graining the scalar field. A scale-local density measure has been introduced to quantify the contributions, as a function of scale, to the coarse-grained interfacial thickness. The data indicate self-similarity in the scale-local interfacial thickness density. A resulting power-law dependence on resolution scale is exhibited by the mean coarse-grained interfacial thickness. This observation of self-similarity, along with other scaling results (e.g. Sreenivasan 1991, 1999), can be expected to be helpful in studies of large-Reynolds-number flows. By combining with knowledge of area-volume properties (e.g. Catrakis *et al.* 2002*a*), the present finding of self-similarity in the interfacial thickness density provides a means to incorporate the dependence on scale in studies of phenomena sensitive to turbulent interfaces (e.g. Pope 1988; Sreenivasan 1991, 1999; Catrakis 2004).

We are grateful for the support of the Air Force Office of Scientific Research, the Defense University Research and Instrumentation Program, and the National Science Foundation. We are also grateful to D. Dunn-Rankin, S. Elghobashi, C. Friehe, and J. LaRue for useful advice as well as to the Referees for their insightful comments.

REFERENCES

Anselmet, F., Djeridi, H. & Fulachier, L. 1994 Joint statistics of a passive scalar and its dissipation in turbulent flows. *J. Fluid Mech.* **280**, 173–197.

Antonia, R. A. & Sreenivasan, K. R. 1977 Log-normality of temperature dissipation in a turbulent boundary layer. *Phys. Fluids* **20**, 1800–1804.

Bilger, R. W. 2004 Some aspects of scalar dissipation. *Flow, Turbulence, & Combustion* **72**, 93–114.

Bisset, D. K., Hunt, J. C. & Rogers, M. M. 2002 The turbulent/non-turbulent interface bounding a far wake. *J. Fluid Mech.* **451**, 381–410.

Brethouwer, G., Hunt, J. C. R. & Nieuwstadt, F. T. M. 2003 Micro-structure and Lagrangian statistics of the scalar field with a mean gradient in isotropic turbulence. *J. Fluid Mech.* **474**, 193–225.

Catrakis, H. J. 2000 Distribution of scales in turbulence. *Phys. Rev.* E **62**, 564–578.

Catrakis, H. J. 2004 Turbulence and the dynamics of fluid interfaces with applications to mixing and aero-optics. In *Recent Research Developments in Fluid Dynamics Vol. 5* (ed. N. Ashgriz & R. Anthony), pp. 115–158. Kerala, India: Transworld Research Network Publishers.

Catrakis, H. J., Aguirre, R. C. & Ruiz-Plancarte, J. 2002*a* Area–volume properties of fluid interfaces in turbulence: scale-local self-similarity and cumulative scale dependence. *J. Fluid Mech.* **462**, 245–254.

Catrakis, H. J., Aguirre, R. C., Ruiz-Plancarte, J., Thayne, R. D., McDonald, B. A. & Hearn, J. W. 2002*b* Large-scale dynamics in turbulent mixing and the three-dimensional space-time behaviour of outer fluid interfaces. *J. Fluid Mech.* **471**, 381–408.

Corrsin, S. & Kistler, A. L. 1955 Free-stream boundaries of turbulent flows. *NACA TR* 1244.

Dahm, W. J. A. & Southerland, K. B. 1997 Experimental assessment of Taylor's hypothesis and its applicability to dissipation estimates in turbulent flows. *Phys. Fluids* **9**, 2101–2107.

Dimotakis, P. E. 2005 Turbulent mixing. *Annu. Rev. Fluid. Mech.* **37**, 329–356.

Friehe, C. A., Van Atta, C. W. & Gibson, C. H. 1971 Jet turbulence: Dissipation rate measurements and correlations. *AGARDograph* CP 93, No. 18, pp. 88–103.

Joseph, D. D. & Preziosi, L. 1989 Heat waves. *Rev. Mod. Phys.* **61**, 41–73.

Kuznetsov, V. R. & Sabel'nikov, V. A. 1990 *Turbulence and Combustion*. Hemisphere.

LaRue, J. C. & Libby, P. A. 1975 Temperature and intermittency in the turbulent wake of a heated cylinder. *Phys. Fluids* **17**, 873–878.

Latz, M. I., Juhl, A. R., Ahmed, A. M., Elghobashi, S. E. & Rohr, J. 2004 Hydrodynamic stimulation of dinoflagellate bioluminescence: a computational and experimental study. *J. Expl Biol.* **207**, 1941–1951.

Meneveau, C. & Katz, J. 2000 Scale-invariance and turbulence models for large-eddy simulation. *Annu. Rev. Fluid. Mech.* **32**, 1–32.

Meneveau, C. & Sreenivasan, K. R. 1991 The multifractal nature of turbulent energy dissipation. *J. Fluid Mech.* **224**, 429–484.

Pope, S. B. 1988 Evolution of surfaces in turbulence. *Intl J. Engng Sci.* **26**, 445–469.

Pope, S. B. 2000 *Turbulent Flows*. Cambridge University Press.

Pullin, D. I. & Saffman, P. G. 1998 Vortex dynamics in turbulence. *Annu. Rev. Fluid. Mech.* **30**, 31–51.

Roshko, A. 1991 The mixing transition in free shear flows. In *The Global Geometry of Turbulence* (ed. J. Jiménez), pp. 3–11. Plenum.

Schumacher, J. & Sreenivasan, K. R. 2003 Geometric features of the mixing of passive scalars at high Schmidt numbers. *Phys. Rev. Lett.* **91**, 4501–4504.

Schumacher, J., Sreenivasan, K. R. & Yeung, P. K. 2005 Very fine structures in scalar mixing. *J. Fluid Mech.* **531**, 113–122.

Sreenivasan, K. R. 1985 On the fine-scale intermittency of turbulence. *J. Fluid Mech.* **151**, 81–103.

Sreenivasan, K. R. 1991 Fractals and multifractals in fluid turbulence. *Annu. Rev. Fluid. Mech.* **23**, 539–600.

Sreenivasan, K. R. 1999 Fluid turbulence. *Rev. Mod. Phys.* **71**, S383–S395.

Sreenivasan, K. R. 2004 Possible effects of small-scale intermittency in turbulent reacting flows. *Flow, Turbulence, & Combustion* **72**, 115–141.

Sreenivasan, K. R., Prabhu, A. & Narasimha, R. 1983 Zero-crossings in turbulent signals. *J. Fluid Mech.* **137**, 251–272.

Sreenivasan, K. R., Ramshankar, R. & Meneveau, C. 1989 Mixing, entrainment and fractal dimensions of surfaces in turbulent flows. *Proc. R. Soc. Lond.* A **421**, 79–108.

Su, L. K. & Clemens, N. T. 1999 Planar measurements of the full three-dimensional scalar dissipation rate in gas-phase turbulent flows. *Exps. Fluids* **27**, 507–521.

Trouvé, A. & Poinsot, T. 1994 The evolution equation for the flame surface density in turbulent premixed combustion. *J. Fluid Mech.* **278**, 1–31.

Villermaux, E. & Innocenti, C. 1999 On the geometry of turbulent mixing. *J. Fluid Mech.* **393**, 123–147.

Warhaft, Z. 2000 Passive scalars in turbulent flows. *Annu. Rev. Fluid. Mech.* **32**, 203–240.